INSTITUTE OF PHYSICS PUBLISHING JOURNAL OF PHYSICS: CONDENSED MATTER

J. Phys.: Condens. Matter **14** (2002) 4645–4657 PII: S0953-8984(02)33405-2

Real-space rigid-unit-mode analysis of dynamic disorder in quartz, cristobalite and amorphous silica

Stephen A Wells, Martin T Dove, Matthew G Tucker and Kostya Trachenko

Mineral Physics Group, Department of Earth Sciences, University of Cambridge, Downing Street, Cambridge CB2 3EQ, UK

Received 4 February 2002, in final form 2 April 2002
Published 26 April 2002
Online at stacks.iop.org/JPhysCM/14/4645

Abstract

We use a recently developed tool based on geometric algebra to analyse the phase transition in quartz, the nature of the disordered high-temperature phase of cristobalite and the dynamics of silica glass. The approach is to analyse configurations generated by the reverse Monte Carlo or molecular dynamics simulations in terms of rigid-unit-mode (RUM) motions, but concentrating on quantifying the real-space distortions rather than performing a reciprocal-space analysis in terms of RUM phonons. One of the important results is a measure of the extent to which the amplitudes of motion are directly attributable to RUMs, and how the RUM fraction changes as a result of a phase transition.

(Some figures in this article are in colour only in the electronic version)

1. Introduction

Some understanding of the displacive phase transitions in framework materials, namely materials whose crystal structures can be described as frameworks of connected polyhedral groups of atoms, has been attained on the basis of the rigid-unit-mode (RUM) model [1,2]. The essence of this model is to recognize that the energy cost associated with the deformation of a structural polyhedron is much higher than the energy change due to swinging two polyhedra about a common vertex. As a result, a displacive phase transition is more likely to occur if the framework can distort without the individual polyhedra having to be deformed. The well known octahedral tilting phase transitions in perovskites (see figure 1) are representative examples of this idea, but the greatest progress in applying the RUM model has come in the study of silicates composed of corner sharing SiO_4 and AlO_4 tetrahedra. Classic examples are the phase transitions in quartz and cristobalite [3].

The RUM model has been formulated in terms of phonon modes, so it is a reciprocal space picture. An algorithm, known as the 'split-atom model', has been developed to allow the calculation of all phonon modes that propagate without deformations of the polyhedra, the so-called RUMs [1,3]. Because RUMs have low energy (typically of order 1 THz or less), the RUMs are natural candidates as soft modes for displacive instabilities. This point has been

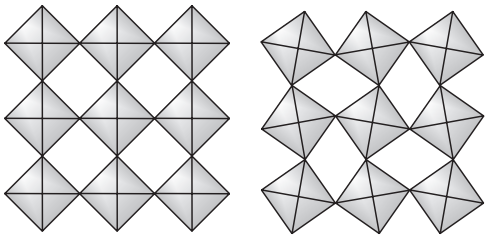

Figure 1. The octahedral rotation mode in the perovskite structure is an example of a RUM.

well documented for quartz [4]. The other important issue is that the high-symmetry phase of a material typically has many more RUMs than its low-symmetry phase. Because RUMs have low frequencies, they will have high amplitudes, scaling as T/ω^2. It is therefore to be expected that a significant part of the dynamics of high-symmetry phases will be dominated by the RUM contribution. Indeed, in cristobalite it has been proposed that the considerable degree of structural disorder seen in the high-temperature phase can be fully explained by this mechanism [5, 6]. Recent RMC studies of the phase transition in quartz have also suggested that the phase transition allows the excitation of more RUMs, which give the appearance of dynamic disorder [7].

The reciprocal-space analysis of structural fluctuations is useful, but not without limitations. In particular, the modes which are active in a real material do not fall neatly into a family of RUMs consisting entirely of displacements and rotations of the tetrahedra, and another family of non-RUMs consisting entirely of distortions of the tetrahedra. Instead, any mode can include components of displacive, rotational and distortive motion, with the relative proportions of the different types varying more or less continuously from low-frequency modes with little distortive component to high-frequency modes with little rigid-unit component. We have therefore recently developed a real-space analysis of RUM fluctuations [8] based on the technique of geometric algebra (GA) [9, 10]. This allows us to determine the extent to which an instantaneous 'snapshot' of an atomic configuration can be described in terms of RUM displacements, by decomposing the motion into displacive, rotational and distortive motion. In fact this approach is providing the first quantitative analysis of the effects of RUMs on creating dynamic disorder in crystals.

Our purpose in this paper is to combine our GA RUM analysis with the results of reverse Monte Carlo (RMC) simulations of the phase transition in quartz to provide a detailed understanding of the changes in the RUM spectrum through the phase transition. This will properly quantify the discussion of the role of RUMs in the phase transition. We also extend the analysis to studies of the dynamics of cristobalite and amorphous silica.

2. Fitting a rotation

To quantify the effect of RUMs we make use of the bond vectors within each polyhedron. Let us suppose that we have two slightly different forms of the same structure, in which the atoms have shifted slightly and the polyhedra have different orientations but no bonds have broken or formed. For each bond we have a vector from the central atom p to an atom q at a vertex of the polyhedron; for one form of the structure let us call this vector PQ, for the other form PQ'. For example, PQ might be the bond vectors in an ideal structure with perfectly regular tetrahedra, while PQ' might be a snapshot of the dynamic disorder in this structure; or both PQ and PQ' may be snapshots of the system in different states. Our assumption, from the rigid-unit picture, is that there exists a rotation of the polyhedron p which takes the set of vectors PQ very close to PQ'.

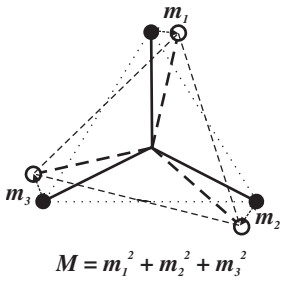

Figure 2. The best-fit rotation is that which minimizes the mismatch value M.

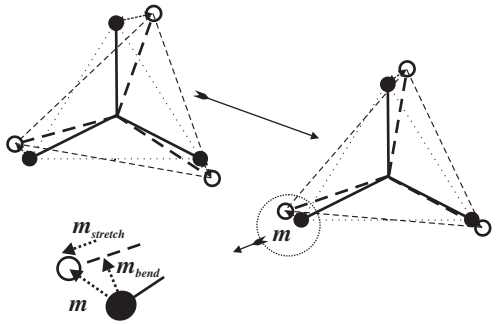

Figure 3. Where both rotation and distortion are present, there will be some residual mismatch, which can be divided into bending and stretching terms.

2.1. Mismatch equation

We can write down a vector $PQ''(PQ, R)$, representing the vector PQ after the rotation defined by R; this allows us to write a mismatch vector E, given by $E_q = PQ'' - PQ'$. Minimizing this mismatch with respect to the parameters of a rotation will give the rotation which best fits PQ onto PQ'. This is illustrated in figure 2.

If the bond lengths $l_{PQ}, l_{PQ'}$ differ, than a part of the residual distortion can be attributed to a bond-stretching term. The remainder of the distortion is due to flexing of the tetrahedral angles. So long as the flexions are small then the bond-stretching and bond-angle-bending displacements of the atom Q are approximately orthogonal to each other, so that we may divide the residual distortion $E^2_{q,\text{after}}$ into bending and stretching terms, thus: $E^2_{q,\text{after}} = m^2_{\text{bend}} + m^2_{\text{stretch}}$. This is illustrated in figure 3.

We define a mismatch score M for the polyhedron by summing the squares of the mismatch vectors E_q over all the bonds in a polyhedron:

$$M = \sum_q E_q^2. \tag{1}$$

Usually $q = 4$ as we are often dealing with SiO_4 tetrahedra.

We can take M as a function over a vector space whose basis is the parameters of the rotation. In a previous paper [8] we showed that the formalism of GA [9, 10] gives a very convenient parametrization of a rotation, giving us an explicit algebraic expression for M which can easily be differentiated by the parameters to give ∇M.

To find the minimum of M we use the method of steepest descents, starting from a zero rotation and taking steps in the direction of $-\nabla M$ until $|\nabla M|$ is sufficiently close to zero to

be considered a minimum. This gives the best-fit rotation for the polyhedron and the value of M at the minimum represents the residual distortion of the polyhedron.

In this analysis we are clearly taking the displacement of the tetrahedron to be the displacement of the central atom, which is implicitly subtracted from our analysis when we take the bond vectors relative to the central atom. Our discussions of disorder hereafter focus on the orientational (rotational and distortive) disorder of the tetrahedra.

3. Reverse Monte Carlo modelling

Recently we have carried out a series of RMC studies on framework silica structures [6, 7]. These have been based on neutron total scattering studies performed at the ISIS spallation neutron source. The RMC method was modified to account explicitly for the Bragg peaks [11]. As a result, the RMC simulations are designed to account for both short- and long-range order, and will highlight how fluctuations of the structure give short-range structures that differ from the average structure of the long-range order.

The RMC method is used to generate configurations of atoms that are consistent with the total scattering data. In our case, this means that the configurations are consistent with the total scattering intensity, the pair distribution functions and the intensities of the Bragg peaks.

In our study of quartz [6], measurements were performed over a wide range of temperatures below the phase transition temperature, and for some temperatures above the phase transition. The RMC configurations therefore provide information about changes in both short-range and long-range order as a continuous function of temperature on heating through the phase transition. The data on cristobalite are mostly for the high-temperature disordered phase, and as a result it has not been possible to study the phase transition *per se*. Instead, the focus of our attention in this case is the nature of the structural disorder in the high-temperature phase.

Two configurations were generated from the scattering data at each temperature value. Both configurations started with the same initial configuration, but the stochastic nature of the RMC algorithms means that the two configurations differed slightly from each other. We treat the two configurations as two snapshots of the dynamic disorder, and apply our rotor-fitting algorithms, taking the bond vectors PQ from one configuration and PQ' from the other. The initial mismatch score M_{before} before fitting a rotation gives a measure of the total orientational disorder, while the residual mismatch M_{after} after fitting a rotation represents actual tetrahedral distortion; the difference between the two M_{rot} is attributable to rotational motion of the polyhedra.

When we take more than two configurations and compare all the pairs, we find little variation in the results (on the order of tens of Å^2 out of several thousands), indicating that such configurations of several thousand polyhedra each represent a good sample of the disorder. It is however important to be sure that the RMC fitting is correct and fully converged; we have sometimes found configurations to give wildly different results when the RMC run was interrupted before full convergence.

Since the two configurations represent structures with the same topology, but are generated independently, they can be thought of as two snapshots separated by an infinitely long time interval.

4. Quartz

Figure 4 shows the degree of disorder in quartz as a function of temperature. The values given are the mismatch scores M in Å^2, summed over 24 000 bond vectors in 6000 polyhedra.

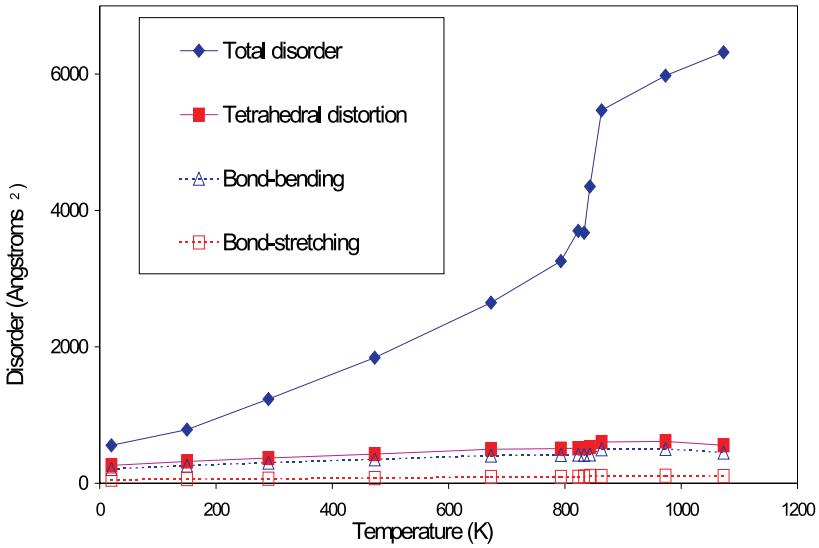

Figure 4. The dynamic disorder in quartz is largely accounted for by rigid-unit motions of the tetrahedra. The difference between the total orientational disorder and the tetrahedral distortion is due to rotational motion. The horizontal axis gives temperature in K; the vertical axis gives mismatch score M in Å^2 summed over 24 000 bond vectors in 6000 polyhedra.

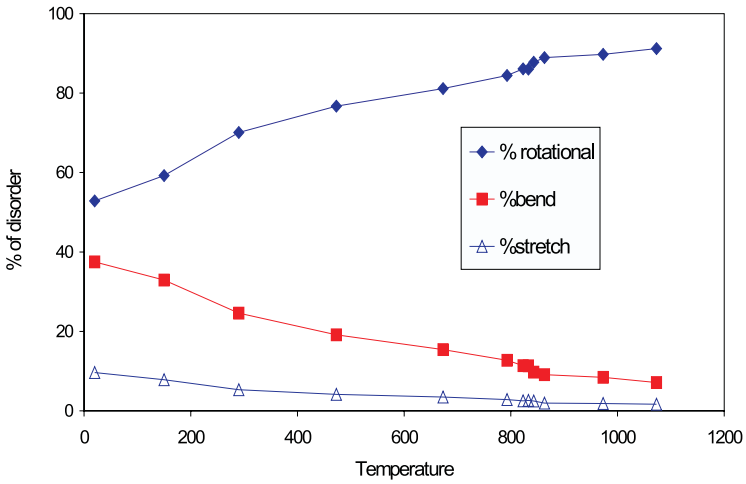

Figure 5. The proportion of the orientational disorder accounted for by rotational motions of the polyhedra increases with temperature, exceeding 90% in the high-symmetry β phase. The horizontal axis gives temperature in K. Proportions are given as percentages of the total orientational disorder at that temperature.

We note first that at room temperature and above the actual tetrahedral distortion is much less than the total orientational disorder. The large difference between the two indicates the contribution of RUMs to the dynamic disorder. Figure 5 gives the rotational contribution as a percentage of the total disorder; this contribution rises from about 70% at room temperature to almost 90% just below the phase transition, and increases above 90% in the β phase. The amplitude of the RUMs increases with temperature much faster than the amplitude of the non-RUM disorder.

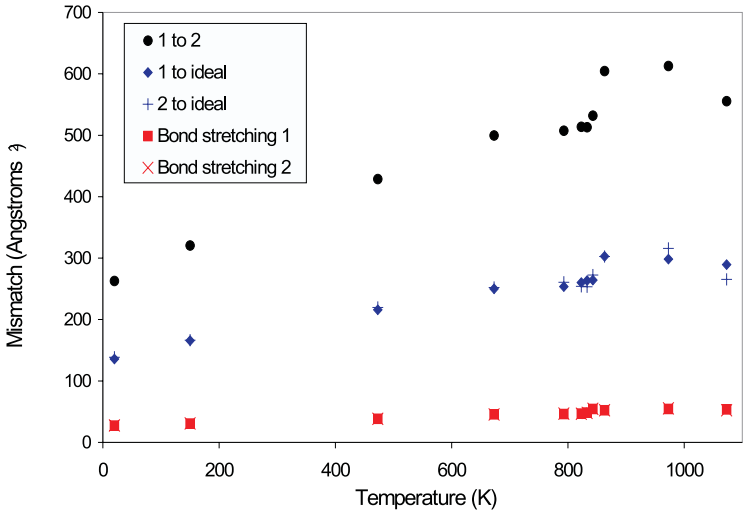

Figure 6. Each of the snapshots can be compared with a framework of ideal tetrahedra. The mismatch between each snapshot and the ideal is approximately half the residual mismatch between one and the other, indicating that the two snapshots represent uncorrelated distortions of the ideal tetrahedra; they represent two states of disorder separated by an infinite time interval. Horizontal axis, temperature in K; vertical axis, total mismatch score in Å^2.

The size of the rotations allowed by rigid-unit motion is striking. A total mismatch score of 6000 Å^2, which is achieved in the β phase, corresponds to a mismatch per bond of 0.25 Å^2. This signifies an RMS displacement of 0.5 Å. Since this mismatch is largely due to rotation, we can estimate the RMS rotation to be about 0.3 rad or 17°, given a bond length of about 1.62 Å.

The tetrahedral distortion can be further divided into the terms due to variation in bond lengths and due to bending of the O–Si–O bond angle. It is clear that the distortion is primarily due to bond bending, with a much smaller bond-stretching component. The nature of the distortions does not appear to change over the temperature range of this study.

Figure 6 shows a comparison of each of the configurations with an ideal framework of tetrahedra; that is, each polyhedron is compared with one with ideal tetrahedral angles and a bond length appropriate to an Si–O bond at that temperature. The resulting mismatch score indicates the degree of distortion of the tetrahedra. The figure shows that the mismatch between each configuration and the ideal is approximately half the residual mismatch between one and the other. Now, the residual mismatch score is a measure of the square of the distance of the atoms from their ideal positions at the vertices of a tetrahedron. The mismatches (1 to ideal) and (2 to ideal) both represent distortions of the ideal tetrahedron. For a given atom, these distortions are two vectors r_1, r_2, giving mismatches r_1^2, r_2^2. The mismatch (1–2) is then given by $(r_1-r_2)^2$. If the average of $(r_1-r_2)^2$ is equal to the average of $r_1^2+r_2^2$, then there is no correlation between the directions of r_1 and r_2. This fits well with our conception of the two configurations representing snapshots of the disorder taken at two widely separated moments in time.

It is known that at low temperatures the polyhedra in quartz are distorted from their geometrically perfect forms, and indeed we can see in figure 6 that the distortion of our configurations relative to geometrically perfect tetrahedra does not tend to zero as temperature tends to 0 K, but rather tends to a value of about 120 Å^2. This would indicate that on average the oxygen atoms are about 0.07 Å from the geometrically ideal position. The distortions of the two different configurations, however, remain uncorrelated.

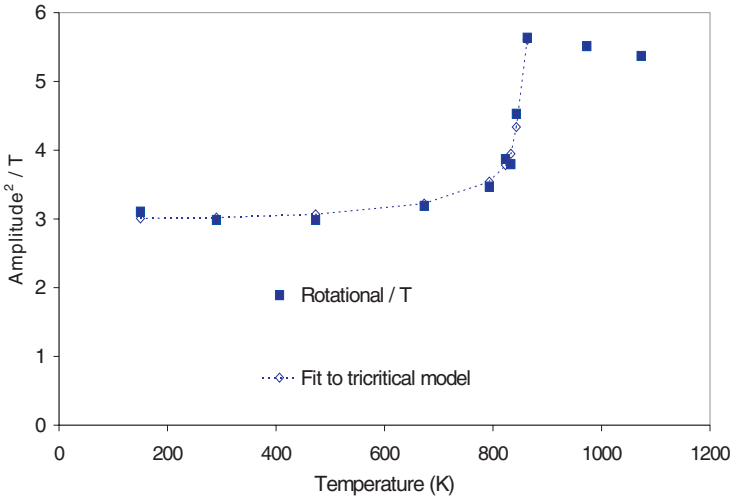

Figure 7. The drop in RUM amplitude due to the α–β phase transition is well fitted by a model in which a fraction $f_{\rm rum}$ of the RUMs from the β phase keep the same frequency $\omega_{\rm rum}$ in the α phase, while the frequency of the remaining fraction $(1 - f_{\rm rum})$ increases by $\Delta\omega = K(T_c - T)^{\frac{1}{4}}$. For this fit $f_{\rm rum} = 0.22$, $\omega_{\rm rum} \approx 1.2$ THz, $K \approx 0.19$. Horizontal axis, temperature in K; vertical axis, $\frac{M_{\rm rot}}{T}$.

4.1. Order parameter

The α–β phase transition is clearly visible in the dynamic disorder, which drops dramatically as the temperature falls below the transition temperature. This is almost entirely due to the effect of the phase transition on the RUMs, as the tetrahedral distortion is almost insensitive to the phase transition. There exist phonon modes which are RUMs in the high-symmetry β phase, involving displacements and rotations of the tetrahedra, but which develop a component of tetrahedral distortion in the low-symmetry α phase. This change is accompanied by a dramatic decrease in amplitude, as the energy cost of the distortion increases the frequency of the mode. We attribute the changes in dynamic disorder with temperature to the effects of the symmetry change on the RUM phonons and the resulting loss of rotational amplitude.

To find a simple interpretation of our data in terms of the effect of the phase transition, we take the mismatch scores $M_{\rm rot}$ to be a measure of the mean squared amplitude $\langle\theta^2\rangle$ of the active RUMs. A simple Einstein model suggests that

$$\langle\theta^2\rangle \propto \sum_{RUMmodes} \frac{T}{\omega^2_{mode}} \tag{2}$$

and we therefore plot $\frac{M_{\rm rot}}{T}$ against T to observe the behaviour of the RUM frequencies. These data are presented in figure 7.

The split-atom model [1] would suggest that, as the average tilt $|\phi|$ of the polyhedra relative to their positions in the β phase increases from zero, some modes which are RUMs in the β phase gain frequency in proportion to $\sin|\phi|$ as they develop a component of tetrahedral distortion. Since the phase transition in quartz is of almost tricritical character, and we do not approach the phase transition closely enough to observe any first-order discontinuity, we take it that

$$|\phi| \propto (T_c - T)^{\frac{1}{4}}. \tag{3}$$

We therefore adopt a model in which a fraction $f_{\rm rum}$ of the RUMs from the β phase remain true RUMs in the α phase, keeping the same frequency $\omega_{\rm rum}$, while the remaining fraction

$(1 - f_{\text{rum}})$ develop a component of tetrahedral distortion and their frequency increases by $\Delta\omega = K(T_c - T)^{\frac{1}{4}}$. This increase in frequency then leads to a decrease of rotational amplitude as given by the Einstein model above. We fitted this model to our data taking f_{rum}, ω_{rum} and K as parameters, calculating the expected form of the graph of $\frac{M_{\text{rot}}}{T}$ against T for a given set of values of these parameters and finding the values which gave the best fit to the data as measured by the least squared value of the difference between calculated values and data points.

For this fit the optimum values were $f_{\text{rum}} = 0.22$, $\omega_{\text{rum}} \approx 1.2$ THz, $K \approx 0.19$, with $T_c = 860$ K. The fit was quite loose, as ω_{rum} and K can vary together without seriously affecting the fit, although f_{rum} was quite strongly constrained. This is reasonable given that our simple model does not take into account such factors as variations in the moment of inertia of the polyhedra. In any case, the functional form appears to be correct.

The idea that the number of RUMs in a system changes as a result of a phase transition was recognized with the first RUM calculations, and has been attributed to the change in symmetry [1–3]. Moreover, this idea has been used to explain the large temperature dependence of some of the phonons in quartz measured by inelastic neutron scattering. It is useful to compare the quantitative analysis presented here with the direct calculations of the RUM spectrum by the split-atom method. This approach is used to generate a density of states [13]. Because the split-atom method does not include forces other than those that prevent deformations of polyhedra, the RUMs have zero frequencies, and the densities of states do not fall to zero as $\omega \to 0$. This contrasts with the normal Debye ω^2 form of the density of states at low ω. In fact, the size of the low-ω split-atom density of states provides a quantitative measure of the RUM flexibility of a structure.

We have used this approach to estimate the inherent RUM flexibility of the two phases of quartz. The split-atom densities of states are shown in figure 8. The important point to note is that there is a considerable shift of some of the low-ω density to slightly higher frequencies (in the sub-2 THz regime). It is not realistic to compare this effect directly with our estimate of an effective persistent RUM fraction above, but in general terms the picture that is given by the GA analysis of the RMC configurations is matched in the split-atom analysis.

5. Cristobalite

There is considerable evidence for a high degree of structural disorder in the high-temperature phase of cristobalite [14, 15]. The 'average' structure, namely that obtained by structure refinement from Bragg diffraction data, has the average position of the oxygen atoms lying exactly halfway between its two silicon neighbours. This means a linear Si–O–Si linkage, something that is not common. It is more usual for this linkage to be bent to around 145°. The crystal structure refinements show evidence for large-amplitude motions of the oxygen normal to the axis of the linkage. This can be interpreted as considerable bending of this linkage due to large-amplitude rotations of the SiO_4 tetrahedra [16]. It had been suggested that this could be achieved through the formation of many domains of the low-temperature phase or of another lower-symmetry structure, with these domains switching dynamically to create the average structure. The initial RMC work has subsequently shown that this interpretation is not what is actually happening, and instead an interpretation of the disorder based on the excitation of the RUM spectrum is the more likely explanation. We now use our GA analysis to quantify this idea.

For cristobalite data were available for five temperature points, though since only one lies in the low phase no order-parameter fit is possible. The simulations were carried out on varying numbers of polyhedra (4000 in the low phase and 8000 in the high) but the results

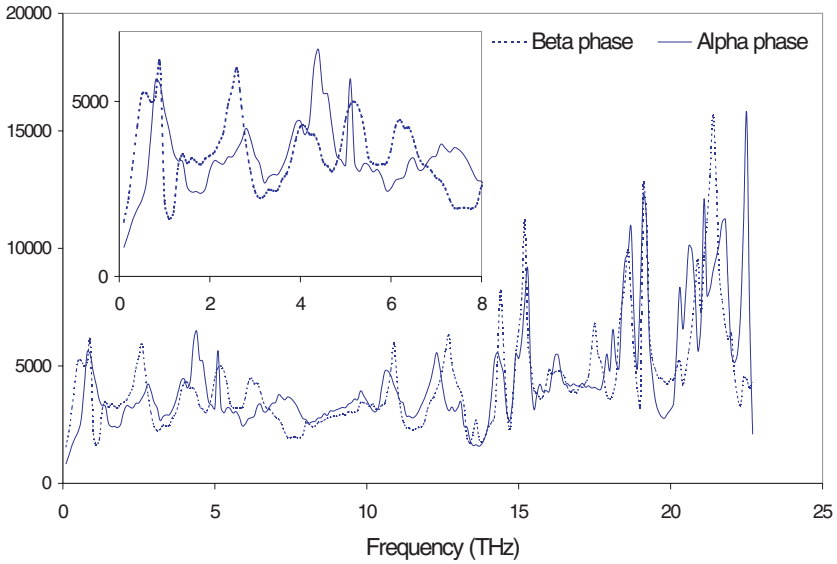

Figure 8. Density of states for quartz from the split-atom model. Horizontal axis, frequency in THz; vertical axis, histogram of $g(\omega)$, arbitrary units. Inset: low-frequency regime showing shift to higher frequencies in α-quartz compared with β-quartz.

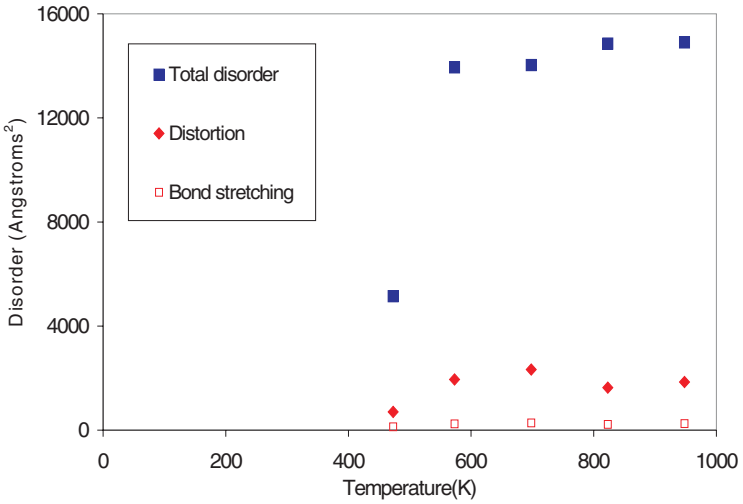

Figure 9. In cristobalite we see the same type of behaviour as for quartz. Note that the disorder in cristobalite is greater than that in quartz, as cristobalite possesses more RUMs.

have been scaled to the equivalent of 6000 polyhedra in all cases to facilitate comparison with the quartz data. The results are plotted in figure 9.

The type of behaviour is the same as in quartz, with a large amount of dynamic disorder in the high phase, dropping rapidly in the low phase, and with most of the disorder being accounted for by RUMs. It is noticeable that the amount of rotational motion in cristobalite is considerably higher than in quartz (approximately twice as much mismatch), indicating that the structure is considerably more flexible.

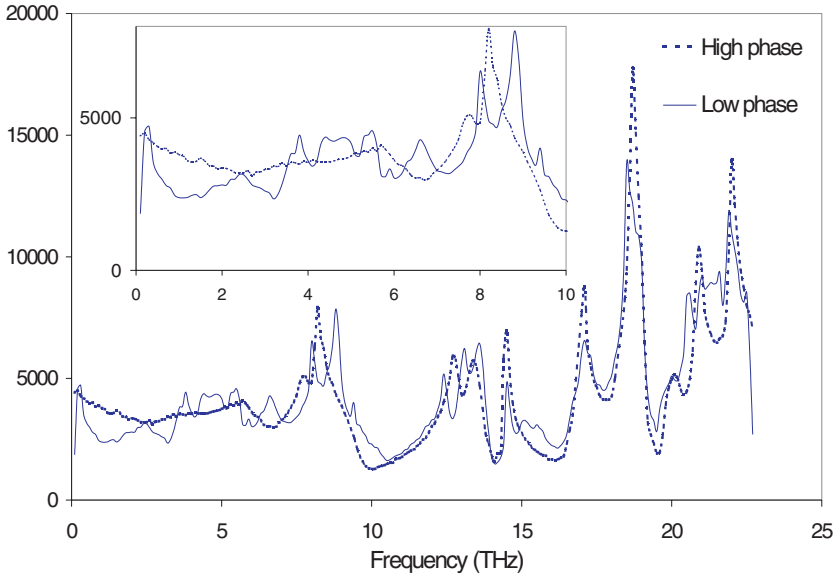

Figure 10. Density of states for cristobalite from the split-atom model. Horizontal axis, frequency in THz; vertical axis, histogram of $g(\omega)$, arbitrary units. Inset: low-frequency regime showing non-Debye dependence at low ω in high cristobalite.

Following the analysis for quartz, we compare our GA analysis with the results of split-atom calculations of the RUM densities of states of the two phases of cristobalite. These are shown in figure 10. It is clear we expect many more RUMs in the high-temperature phase, as shown in our GA analysis. This has been demonstrated by inelastic neutron scattering measurements [6].

6. Dynamic disorder in a glass

We have also applied our analysis to a molecular dynamics simulation of a glass framework, so as to quantify the importance of rigid-unit motion in an amorphous structure [17,18]. This is an interesting case as the origins of flexibility in amorphous frameworks are not well understood. A Maxwell count of the constraints and degrees of freedom in a tetrahedral framework would indicate that the structure was neither floppy nor overconstrained but rather on the boundary between the two, making it difficult to say whether a structure has any RUMs or not. In the case of crystalline structures such as quartz and cristobalite, the symmetry of the structure makes certain constraints redundant leaving the structure underconstrained and allowing RUMs. In the glass, however, it is not clear how the floppy modes arise.

We studied a series of frames from a movie of an MD simulation [18] of SiO_2 glass at 50 K. The frames were spaced 20 MD timesteps apart and we studied some 600 frames, covering 12 000 timesteps. The length of an MD timestep was 0.002 ps, so frames were spaced 0.04 ps apart. This is a very different regime from the RMC simulations which we studied above, as successive frames are very closely spaced in time; the interval between successive frames is considerably less than the period of a RUM. Note that a frame spacing of 0.04 ps is a frame frequency of 25 THz. The simulation included 4096 SiO_2 polyhedra.

Figure 11 shows the results of an analysis in which a frame N was compared with all subsequent frames $N+1$, $N+2$, ... in the movie. The results for frame 51 show the character of the results. The total mismatch is divided into rotational and distortive components. The

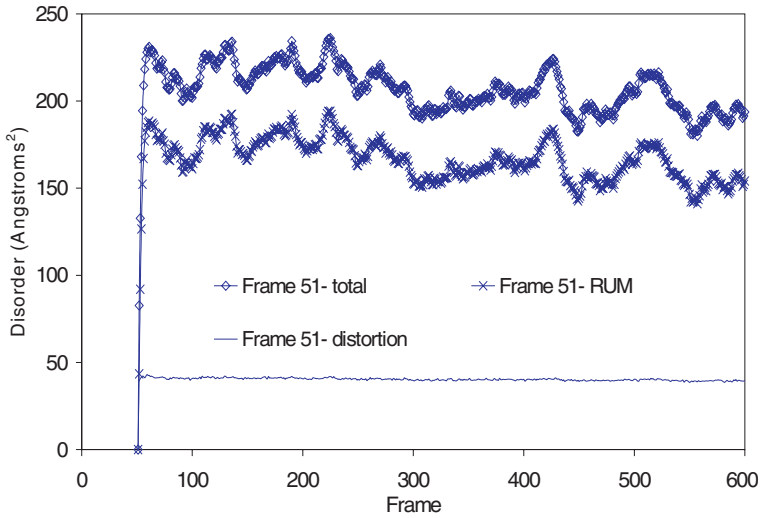

Figure 11. This analysis of a MD simulation of glass shows the action of floppy modes in the structure. Large motions of the structure are accomplished by rotational motion. The distortive component representing high-frequency thermal agitation remains small and roughly constant throughout, whereas the RUM component is large and varies considerably. The mismatch score is summed over 4096 polyhedra at 50 K. Horizontal axis, frame number N; vertical axis, total mismatch score in Å^2 between frame 51 and frame N.

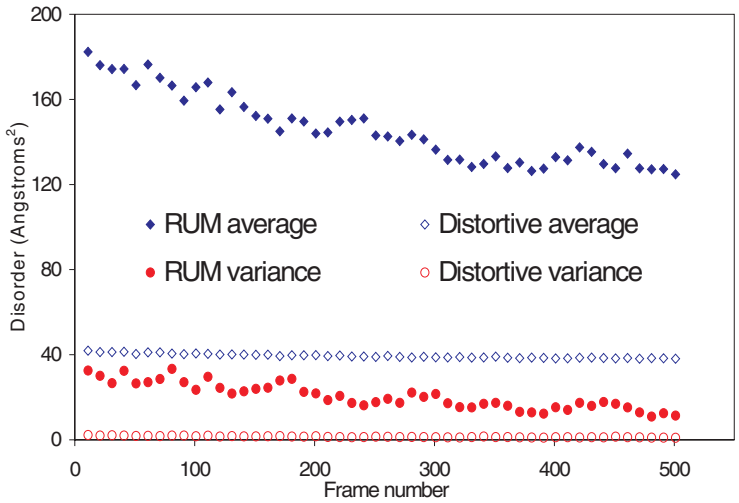

Figure 12. Mean and variance of the rotational and distortive components of the motion. Horizontal axis, starting frame; vertical axis, total mismatch score in Å^2.

distortive component rapidly (within two frames) reaches an equilibrium value and scarcely varies from this value thereafter, regardless of the time interval between frames. We attribute this variation mostly to high-frequency thermal agitation of the structure. The rotational component grows more slowly from zero towards an average value over a space of 10–15 frames, indicating the structure's gradual evolution in phase space. This component also displays much more variation about the mean. This indicates that large-scale reorientations of the structure, achieved by rigid-unit motion, are taking place.

The average size of the rotational component ($\simeq$150 Å^2) is much greater than that of the tetrahedral distortion ($\simeq$40 Å^2) indicating the dominant role of floppy modes in the dynamics of the glass.

Since the time between frames is much less than one period of the floppy modes which are active in the glass, we can observe the gradual growth of the RUM component over some 10 or 15 frames from zero towards a maximum value. Having reached this value, however, the structure does not evolve back along the same path towards a zero RUM mismatch, but instead moves elsewhere in phase space, indicating constant changes in the set of active floppy modes. The large variations in the mismatch score appear to show the gradual evolution of the structure through a phase space defined by rigid-unit motions of the tetrahedra.

For any given frame, we can perform an analysis such as the one given for frame 51. Rather than plot such a graph for each of several hundred frames, we can summarize the results by giving the mean and variance of the rotational and distortive components of the disorder, as shown in figure 12. The mean for frame X was calculated beginning with the comparison with frame X+15, so as not to drag down the average by including the initial gradual rise. Two phenomena are evident. Firstly, the average of the rotational component decreases gradually across the figure, since the distance in phase space from the final configuration is decreasing. Secondly, the RUM component varies considerably as the structure undergoes large reorientations through rigid-unit motion, while the distortive component scarcely varies. This component we ascribe to thermal agitation of the polyhedra by high-frequency modes which do not lead to large atomic motions and whose average remains almost constant over these several thousand polyhedra.

It has been suggested that the low-energy dynamics of glasses involves two-level tunnelling states in localized double-well potentials [19, 20]. Molecular dynamics simulations indicate that large tetrahedral rearrangements can occur at a small energy cost, and these rearrangements have been identified with the existence of double-well potentials [17, 18]. The split-atom model suggests that amorphous silica can support floppy modes analogous to RUMs much as do crystalline silica polymorphs such as cristobalite, and these modes would provide a mechanism for such large tetrahedral rearrangements at low energy cost. Our GA analysis has for the first time quantified the role of rigid-unit motion in these rearrangements.

7. Summary

The GA method for performing a real-space analysis of RUM motions has been applied to a number of systems in this paper. This has enabled us to obtain a quantitative estimate for the fraction of the atomic motions that are due to RUMs. The most extensive data are for quartz, and we have been able to show how the degree of RUM motion changes as a result of the nearly continuous change in structure on cooling through the phase transition. This method has provided the first quantitative measure of the role of RUMs in determining the dynamic disorder in these materials, giving essential support to the interpretation of structural disorder provided by the RUM theory.

Acknowledgments

We are grateful to EPSRC for financial support, and to Michael Carpenter for useful discussions. The molecular dynamics calculations were performed on the computers of the Cambridge High Performance Computing Facility.

References

[1] Giddy A P, Dove M T, Pawley G S and Heine V 1993 The determination of rigid unit modes as potential soft modes for displacive phase transitions in framework crystal structures. *Acta Crystallogr.* A **49** 697–703

[2] Dove M T, Trachenko K O, Tucker M G and Keen D A 2000 Rigid Unit Modes in framework structures: theory, experiment and applications *Rev. Mineral. Geochem.* **39** 1–33

[3] Hammonds K D, Dove M T, Giddy A P, Heine V and Winkler B 1996 Rigid unit phonon modes and structural phase transitions in framework silicates *Am. Mineral.* **81** 1057–79

[4] Vallade M, Berge B and Dolino G 1992 Origin of the incommensurate phase of quartz. 2. Interpretation of inelastic neutron-scattering data *J. Physique* I **2** 1481–95

[5] Gambhir M, Dove M T and Heine V 1999 Rigid unit modes and dynamic disorder: SiO_2 cristobalite and quartz *Phys. Chem. Min.* **26** 484–95

[6] Tucker M G, Squires M D, Dove M T and Keen D A 2001 Dynamic structural disorder in cristobalite: neutron total scattering measurement and reverse Monte Carlo modelling *J. Phys.: Condens. Matter* **13** 403–23

[7] Tucker M G, Dove M T and Keen D A 2000 Simultaneous analyses of changes in long-range and short-range structural order at the displacive phase transition in quartz *J. Phys.: Condens. Matter* **12** 723–30

[8] Wells S A, Dove M T and Tucker M G 2002 Finding best-fit polyhedral rotations with geometric algebra *J. Phys.: Condens. Matter* **14** 4567–84

[9] Lasenby J, Lasenby A N and Doran C J L 2000 A unified mathematical language for physics and engineering in the 21st century *Phil. Trans. R. Soc.* A **358** 21–39

[10] The Geometric Algebra Research Group home page http://www.mrao.cam.ac.uk/ clifford/

[11] Tucker M G, Dove M T and Keen D A 2001 Application of the reverse Monte Carlo method to crystalline materials *J. Appl. Crystallogr.* **34** 630–8

[12] Carpenter M A, Salje E K H, Graeme-Barber A, Wruck B, Dove M T and Knight K S 1998 Calibration of excess thermodynamic properties and elastic constant variations due to the α–β phase transition in quartz *Am. Mineral.* **83** 2–22

[13] Hammonds K D, Dove M T, Giddy A P and Heine V 1994 CRUSH: a FORTRAN program for the analysis of the rigid unit mode spectrum of a framework structure *Am. Mineral.* **79** 1207–9

[14] Swainson I P and Dove M T 1993 Low-frequency floppy modes in β-cristobalite *Phys. Rev. Lett.* **71** 193–6

[15] Swainson I P and Dove M T 1995 Molecular dynamics simulation of α- and β-cristobalite *J. Phys.: Condens. Matter* **7** 1771–88

[16] Dove M T, Keen D A, Hannon A C and Swainson I P 1997 Direct measurement of the Si–O bond length and orientational disorder in β-cristobalite *Phys. Chem. Min.* **24** 311–17

[17] Trachenko K, Dove M T, Hammonds K D, Harris M J and Heine V 1998 Low-energy dynamics and tetrahedral reorientations in silica glass *Phys. Rev. Lett.* **81** 3431–4

[18] Trachenko K, Dove M T, Harris M J and Heine V 2000 Dynamics of silica glass: two-level tunnelling states and low-energy floppy modes *J. Phys.: Condens. Matter* **12** 8041–64

[19] Anderson P W, Halperin B I and Varma C M 1972 *Phil. Mag* **25** 1

[20] Philips W A 1972 *Low Temp. Phys.* **7** 351